RSC Advances

ROYAL SOCIETY OF CHEMISTRY

www.rsc.org/advances

Graphical Abstract

Chalcomer assembly of optical chemosensors for selective Cu^{2+} and Ni^{2+} ion recognition

Gurjaspreet Singh,* Jandeep Singh, Satinderpal Singh Mangat, Jasbhinder Singh

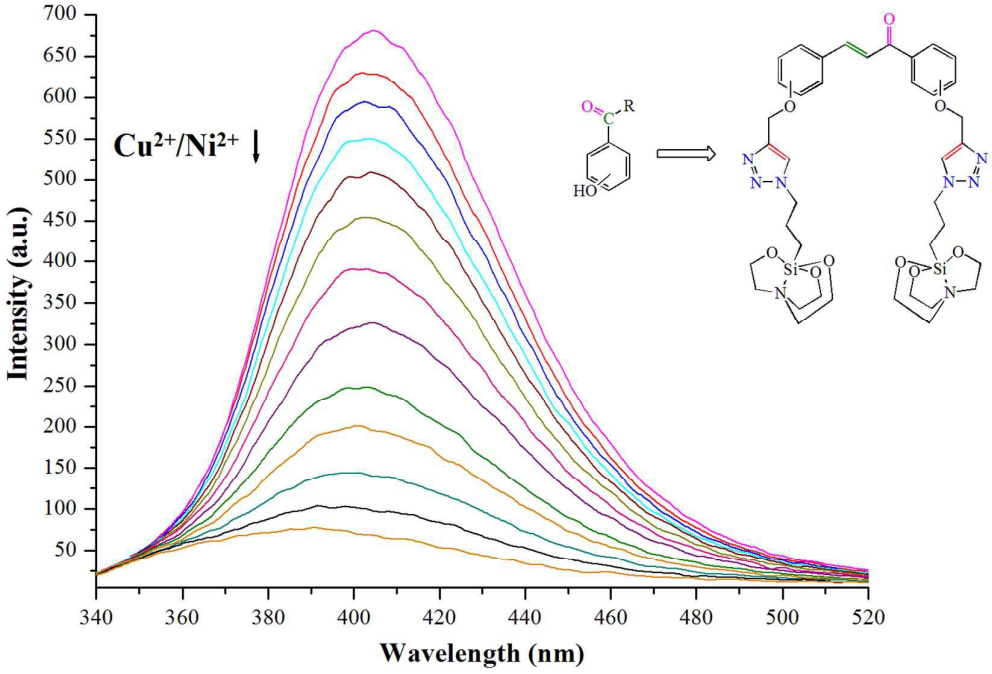

Chalcomer assembly of optical chemosensors for selective Cu^{2+} and Ni^{2+} ion recognition

Gurjaspreet Singh,* Jandeep Singh, Satinderpal Singh Mangat, Jasbhinder Singh, Sunita Rani

Department of Chemistry and Centre of Advanced Studies, Panjab University, Chandigarh, 160014, India.

*Corresponding Author

Email: gjpsingh@pu.ac.in, Phone: +91-0172-2534428

Abstract

The o-, m- and p-isomeric units of chalconyl triazole based caged organosilicon complexes were efficiently synthesized, and explored for the cationic chemosensing activities. The UV–Vis spectral studies performed illustrate considerable variations in absorption spectra and molar absorptivity constant. The recognition studies display efficient sensing for o-isomer of chalcone linked 1,2,3–triazole silatranes isomers (CTSI) **1–3** and acts as dual ion fluorescent sensor towards Cu^{2+} and Ni^{2+} ions. This preferentiality of o-isomers (**CTSI 1–3**) over m- and p-isomers (**CTSI 4–9**) in quenching is due to specific 'fitting in' of coordination sphere available for ion binding. Further, the exceptional activity of **CTSI 8** to exclusively sense Ni^{2+} ions differs from other studied quenching response patterns, which acts by 'turn-on' fluorescence response. The variation of pH and temperature on chemosensing behavior of **CTSI 1–3** led us to optimize conditions for quenching studies. Moreover, the competitive quenching studies confirm feebly enhanced selectivity of Cu^{2+} over Ni^{2+} ions. Stern–Volmer constant (K_{SV}) for all active isomers show comparative quenching response towards both cationic species. This is for first the time for organosilicon complexes to actively sense Cu^{2+} and Ni^{2+} ions using water as one of the solvent mixture.

Keywords:

Positional isomerism, Fluorescence study, Click Chemistry, Cu^{2+} and Ni^{2+} sensors, Quenching response

Introduction

Isomers continue to be an area of keen interest and play fundamental role in the efficient functioning of living systems.[1] The variation in chemical properties of isomeric units is regulated by the difference in their reactivity and interaction with substrates entities. This effect can be best illustrated as; one isomer of dietary ingredient acts as an active and medicinally essential pharmacore while its isomeric forms may be potentially fatal.[2] This utility of isomers draw a parallel analogy to biomolecules which operate by 'lock and key mechanism' and operates via 'on–off' activity.[3] The analytical challenge imposed by difference in activity of isomeric units present a major implication in growing biological applications. Moreover, the importance of isomers in qualitative and quantitative detection of excess metal ions, by fluorescent recognition studies is little explored and forms an area of uprising concern in ion detection therapeutic studies.[4,5]

Chemosensors form robust and consistent molecular tools and have been extensively used in detection of environmental pollutants, such as toxic metals and act as biological markers in medical diagnostic studies.[6–8] The ion detecting property of a fluorescent chemosensor is based upon host–guest relationship in a way the receptor is linked to fluorophore in recognition process.[9] This 'host' component is covalently or coordinate covalently linked to 'guest' module and the complexation with target metal ion results into variation of either intensity or position of emission band for chem–fluorophore.[10] The specificity and selectivity of a receptor to bind target imparts singularity to every sensor.[11] The selective recognition of target multivalent transition metals by chemosensors has attracted considerable attention due to increasing concerns on human health and environmental safety.[12,13] Heavy metal ions like Cd^{2+}, Cu^{2+}, Hg^{2+}, Pb^{2+}, Ni^{2+}, Fe^{2+}, Al^{3+} and Zn^{2+} form major component of environmental pollutants that indirectly affect organisms with serious health disorders. Therefore, the

qualitative and quantitative detection of these toxic elements is must for proper treatment of these toxic contaminants.[14]

Copper and nickel are among the crucial transition metal ions for living systems that help in proper enzyme functioning and facilitate effective iron absorption.[15] Cu (II) acts as cofactor for numerous metalloenzymes whereas Ni (II) assists in iron uptake from intestine, that regulates cellular energy level and maintains metabolic homeostasis. The exposure to slight excess of these cations can cause major syndromes such as Menke's disease, Wilson's disease, Alzheimer disease and gastro-intestinal disorder leading to liver or kidney damage.[16] Designing of new fluorogenic chemosensors for the active recognition of these excess cations with good emission wavelength, and optical stability is must to regulate the toxicity levels. Many systems have been reported, citing the fluorescence sensing of Cu^{2+} and Ni^{2+} ions independently which is based upon binding capability of various chelating agents.[17–19] Recently, there has been a great interest on chemosensing of transition metal ions but limited literature is available for dual sensing for Cu^{2+} and Ni^{2+} ions.[20–23] As a continuous work, nine isomers of triazolyl substituted α, β unsaturated chalcone (chalcomer) backbone are being explored for their fluorogenic receptor properties as dual chemosensor for both Cu^{2+} and Ni^{2+} ions.

Chalcones are α, β unsaturated keto products synthesized by Claisen–Schmidt condensation reaction of aldehydes and ketones. The significant attention on chalcones owe to their wide applicability in medicine as antimalarial, antipathogenic, antitumorigenic, antiinflammatory, antioxidant, antituberculosis, and anti–HIV activities.[24–29] Besides therapeutic effects, chalcones can also act as good chemosensors for various cations due to their conjugate π–electronic system.[30] The exploitation of 'Click Chemistry' to generate active podants that can act as fluorescent potential chemosensors that can be used for the detection of various

transition metal ions above their inhibitory toxic concentration level.[31,32] Moreover, the five membered triazolyl heterocycle is associated with vast applications such as antimycobacterial, antituberculosis, antiangiogenic, antiviral, anticancerous and anti–HIV activity.[33–36] The capping of silicon results into a stable product that increases the applicability of chalcone triazolyl silicon compounds to nanoparticles and biologically active entities.[37–43] In particular, our focus lies on readily available substrates that can undergo transformations to generate chalcone 1,2,3-triazole silatranes isomers **CTSI 1–9** (Scheme 1).

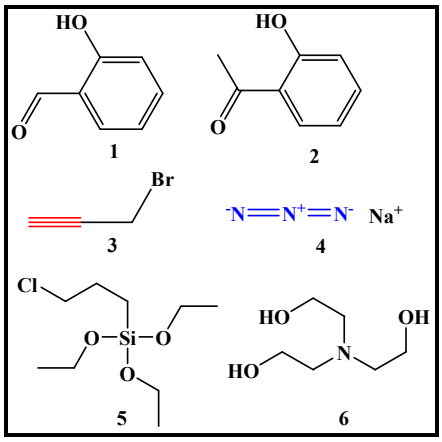

Scheme 1: Entities for generation of chalcomers **1–9**

Experimental

Caution! *Azide compounds are explosive to heat and shock. Great care and protection is required for handling of these compounds.*

General material and methods: All the syntheses were carried out under dry nitrogen atmosphere using vacuum glass line. The organic solvents used were dried and purified according to the standard procedure and stored under dry nitrogen atmosphere. Bromotris(triphenylphosphine)copper(I) (Aldrich), γ-chloropropyltriethoxysilane (ClPTES) (Aldrich), propargyl bromide (80% wt. solution in toluene) (Aldrich), sodium azide

(SDFCL), potassium carbonate (THOMAS BAKER), 2-hydroxyacetophenone (SDFCL), 3-hydroxyacetophenone (SDFCL), 4-hydroxyacetophenone (SDFCL), salicylaldehyde (Aldrich), 3-hydroxybenzaldehyde (SDFCL), 4-hydroxybenzaldehyde (SDFCL) and triethanolamine (SDFCL) were used as supplied for synthesis of compounds **CTSI 1–9**. γ-azidopropyltriethoxysilane (AzPTES) was synthesized according to procedure known in literature.[44]

Melting points were uncorrected and measured in a Mel Temp II device using sealed capillaries. Infrared spectrum was obtained neat on a Thermo Scientific Fischer spectrometer. Multinuclear NMR (^{1}H, ^{13}C) spectra were recorded on a Bruker advance II 400 NMR spectrometer (in $CDCl_3$) at 298K. Mass spectroscopy data of synthesized compounds **CTSI 1** was recorded on Waters QQ–TOF micro Mass Spectrometer. UV–Vis spectra were recorded on JASCO V–530 UV–Vis spectrophotometer. CHN analyses were obtained on a Perkin Elmer Model 2400 CHNS elemental analyser. Fluorescence spectroscopy study was performed on Perkin Elmer LS55 Fluorescence Spectrophotometer.

Synthesis of compounds CTSI 1–9

To the uniformly stirred solution of triethanolamine (1.0 equiv) and potassium hydroxide (cat. amt.) in toluene, slowly added chalcone 1,2,3-triazole triethoxysilane (**C 1–9**) (see supporting information) dropwise within 2 min. The mixture was refluxed for 5 h and after completion, the reaction mixture was cooled to room temperature. The solvent volume in mixture was reduced to 3 mL by vacuum evaporation and addition of 10 mL of n–pentane resulted into separation of slightly coloured solid product. The solid obtained was stirred for 48 h, filtered and washed with 2 x 5 mL n–pentane to afford **CTSI 1–9**.

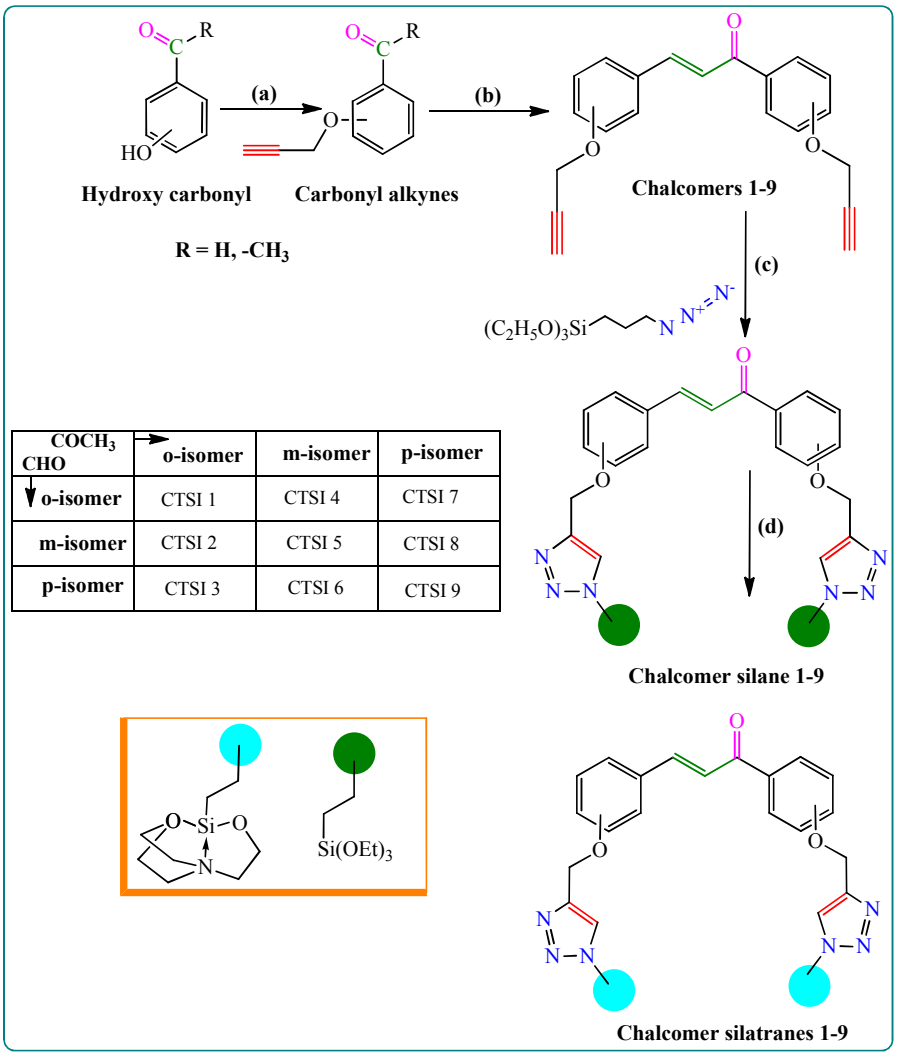

COCH3 / CHO	o-isomer	m-isomer	p-isomer
o-isomer	CTSI 1	CTSI 4	CTSI 7
m-isomer	CTSI 2	CTSI 5	CTSI 8
p-isomer	CTSI 3	CTSI 6	CTSI 9

Scheme 2: Reaction methodology for synthesis of **CTSI 1–9;** Reagents and conditions: a) DMF, propargyl bromide, K_2CO_3, rt, st, 14 h; b) EtOH, KOH, rt, st, 4 h; c) THF:TEA (1:1), [$Cu(PPh_3)_3Br$], 65 ℃, 3 h; d) toluene, triethanolamine, KOH (cat.) 110 ℃, 5 h

Spectroscopic data for compounds CTSI 1–9

1,3-bis(2-(-(1-(3-(silatranyl)propyl)-1H-1,2,3-triazol-4-yl)methoxy)phenyl)prop-2-en-1-one (CTSI 1): Yield: 72%; M. pt. = 130 – 131 ℃ (decom.); Empirical formula: $C_{39}H_{52}N_8O_9Si_2$: Anal. Calcd: C, 56.2; H, 6.3; N, 13.5; Found: C, 56.3; H, 6.2; N, 13.5; IR (neat, cm^{-1}): 2946, 2873, 2807, 1596, 1483, 1448, 1381, 1331, 1237, 1164, 1122, 1096, 989,

909, 850, 753, 681, 616, 583, 541. ^{1}H NMR (400 MHz, $CDCl_3$) δ = 8.12 – 7.99 (m, 1H), 7.88 (d, ^{3}J = 25.6 Hz, 1H), 7.80 (dd, ^{3}J = 18.6, 6.8 Hz, 1H), 7.70 – 7.60 (m, 1H), 7.60 – 7.50 (m, 2H), 7.44 (dd, ^{3}J = 15.1, 10.4 Hz, 1H), 7.27 (d, ^{3}J = 8.5 Hz, 1H), 7.11 – 6.99 (m, 2H), 6.89 – 6.56 (m, 2H), 5.25 – 5.23 (m, 2H), 4.46 – 3.97 (m, 4H), 3.73 – 3.63 (m, 4H), 3.47 (t, ^{3}J = 5.6 Hz, 14H) [2H extra], 2.85 – 2.76 (m, 12H), 2.67 – 2.42 (m, 6H), 1.90 – 1.74 (m, 4H), 0.24 – 0.12 (m, 4H). ^{13}C NMR (101 MHz, $CDCl_3$) δ = 189.37, 164.64, 163.92, 150.45, 144.09, 138.84, 136.04, 135.98, 134.63, 128.54, 127.71, 123.09, 122.90, 120.56, 68.15, 61.15, 58.52, 51.52, 30.19, 13.43. MS (ES^+) Calcd for $[M + Na]^+$ 855.3; Found 855.5.

1-(2-(-(1-(3-(silatranyl)propyl)-1H-1,2,3-triazol-4-yl)methoxy)phenyl)-3-(3-(-(1-(3-(silatranyl)propyl)-1H-1,2,3-triazol-4-yl)methoxy)phenyl)prop-2-en-1-one (CTSI 2): Yield: 76%; M. pt. = 159 – 160 ℃ (decom.); Empirical formula: $C_{39}H_{52}N_8O_9Si_2$: Anal. Calcd: C, 56.2; H, 6.3; N, 13.5; Found: C, 56.2; H, 6.2; N, 13.4; IR (neat, cm^{-1}): 2942, 2873, 2815, 1596, 1482, 1447, 1350, 1236, 1150, 1122, 1095, 973, 909, 851, 751, 680, 616, 580, 540. ^{1}H NMR (400 MHz, $CDCl_3$) δ = 7.58 (dd, ^{3}J = 13.8, 7.4 Hz, 2H), 7.48 (d, ^{3}J = 15.9 Hz, 1H), 7.39 (dd, ^{3}J = 19.2, 11.6 Hz, 2H), 7.32 – 7.13 (m, 2H), 7.05 (dd, ^{3}J = 12.8, 8.3 Hz, 2H), 7.01 – 6.87 (m, 2H), 6.81 (s, 1H), 5.24 (s, 2H), 5.14 (s, 2H), 4.28 (t, ^{3}J = 7.1 Hz, 2H), 4.04 (t, ^{3}J = 7.1 Hz, 2H), 3.68 (t, ^{3}J = 5.8 Hz, 6H), 3.66 (t, ^{3}J = 5.8 Hz, 6H), 2.72 (dt, ^{3}J = 5.8 Hz, 12H), 1.74 – 1.47 (m, 4H), 0.34 – 0.30 (m, 2H), 0.22 – 0.18 (m, 2H). ^{13}C NMR (101 MHz, $CDCl_3$) δ = 198.29, 164.68, 162.91, 148.22, 142.48, 139.22, 138.10, 137.96, 136.62, 135.47, 134.56, 134.44, 133.71, 128.94, 127.50, 127.42, 122.87, 120.18, 119.05, 68.96, 58.38, 51.51, 30.21, 13.36.

1-(2-(-(1-(3-(silatranyl)propyl)-1H-1,2,3-triazol-4-yl)methoxy)phenyl)-3-(-(4-(1-(3-(silatranyl)propyl)-1H-1,2,3-triazol-4-yl)methoxy)phenyl)prop-2-en-1-one (CTSI 3): Yield: 73%; M. pt. = 91 – 92 ℃ (decom.); Empirical formula: $C_{39}H_{52}N_8O_9Si_2$: Anal. Calcd:

C, 56.2; H, 6.3; N, 13.5; Found: C, 56.0; H, 6.3; N, 13.4; IR (neat, cm^{-1}): 2938, 2873, 2807, 1596, 1483, 1447, 1380, 1330, 1237, 1150, 1122, 1096, 988, 909, 850, 752, 680, 617, 581, 541. ^{1}H NMR (400 MHz, $CDCl_3$) δ = 7.74 (d, ^{3}J = 8.7 Hz, 2H), 7.61 (d, ^{3}J = 8.8 Hz, 1H), 7.42 (d, ^{3}J = 15.4 Hz, 2H), 7.35 (d, ^{3}J = 16.2 Hz, 2H), 7.24 (s, 1H), 7.18 (dd, ^{3}J = 9.1, 6.4 Hz, 2H), 7.01 (t, ^{3}J = 6.6 Hz, 2H), 6.92 (d, ^{3}J = 7.8 Hz, 2H), 6.78 (d, ^{3}J = 8.7 Hz, H), 6.74 – 6.67 (m, 3H), 5.01 (d, 2H), 4.98 (d, 2H), 4.49 (t, ^{3}J = 7.1 Hz, 4H), 3.62 (t, ^{3}J = 5.8 Hz, 12H), 2.80 (t, ^{3}J = 5.8 Hz, 12H), 1.79 – 1.72 (m, 4H), 0.30 – 0.26 (m, 4H). ^{13}C NMR (101 MHz, $CDCl_3$) δ = 191.13, 165.74, 162.49, 147.32, 140.50, 136.02, 135.56, 134.65, 133.70, 132.30, 125.90, 120.60, 118.42, 117.86, 66.06, 57.31, 56.11, 51.11, 28.10, 11.33.

3-(2-(-(1-(3-(silatranyl)propyl)-1H-1,2,3-triazol-4-yl)methoxy)phenyl)-1-(3-(-(1-(3-(silatranyl)propyl)-1H-1,2,3-triazol-4-yl)methoxy)phenyl)prop-2-en-1-one (CTSI 4): Yield: 77%; M. pt. = 211 – 213 ℃; Empirical formula: $C_{39}H_{52}N_8O_9Si_2$: Anal. Calcd: C, 56.2; H, 6.3; N, 13.5; Found: C, 56.2; H, 6.4; N, 13.3; IR (neat, cm^{-1}): 2938, 2873, 2811, 1596, 1482, 1447, 1381, 1350, 1236, 1150, 1122, 1096, 974, 909, 851, 751, 680, 615, 582, 540. ^{1}H NMR (400 MHz, $CDCl_3$) δ = 8.01 (dd, ^{3}J = 13.7, 6.7 Hz, 1H), 7.64 – 7.57 (m, 2H), 7.57 – 7.49 (m, 2H), 7.49 – 7.43 (m, 2H), 7.37 (ddd, ^{3}J = 25.9, 7.3, 2.6 Hz, 2H), 7.14 (dt, ^{2}J = 4.6, 3.9 Hz, 1H), 7.09 – 6.91 (m, 2H), 5.24 (s, 2H), 5.17 (s, 2H), 4.29 – 4.24 (m, 4H), 3.69 – 3.65 (m, 12H), 2.73 (q, ^{3}J = 5.8 Hz, 12H), 1.97 – 1.88 (m, 4H), 0.37 – 0.31 (m, 4H). ^{13}C NMR (101 MHz, $CDCl_3$) δ = 191.59, 166.47, 161.56, 146.72, 135.12, 134.00, 133.84, 131.45, 125.84, 124.66, 119.66, 117.27, 116.86, 65.30, 58.49, 58.24, 51.43, 27.40, 10.43.

1-(3-(-(1-(3-(silatranyl)propyl)-1H-1,2,3-triazol-4-yl)methoxy)phenyl)-3-(3-(-(1-(3-(silatranyl)propyl)-1H-1,2,3-triazol-4-yl)methoxy)phenyl)prop-2-en-1-one (CTSI 5): Yield: 77%; M. pt. > 220 ℃; Empirical formula: $C_{39}H_{52}N_8O_9Si_2$: Anal. Calcd: C, 56.2; H, 6.3; N, 13.5; Found: C, 56.1; H, 6.2; N, 13.4; IR (neat, cm^{-1}): 2929, 2873, 2807, 1660, 1578,

1482, 1438, 1381, 1249, 1169, 1122, 1097, 1012, 938, 909, 849, 772, 682, 616, 582, 541. ^{1}H NMR (400 MHz, DMSO) δ = 8.13 (s, 1H), 7.96 – 7.87 (m, 1H), 7.83 – 7.76 (m, 1H), 7.74 (t, ^{2}J = 4.1 Hz, 1H), 7.69 (d, ^{2}J = 4.7 Hz, 1H), 7.65 – 7.59 (m, 2H), 7.54 (dd, ^{3}J = 7.0, 2.3 Hz, 1H), 7.51 – 7.45 (m, 1H), 7.43 (d, ^{3}J = 9.3 Hz, 1H), 7.09 (dd, ^{3}J = 18.2, 6.5 Hz, 2H), 5.24 (s, 1H), 5.21 (s, 1H), 4.89 (s, 1H), 4.86 (s, 1H), 4.24 (dd, ^{3}J = 9.4, 4.5 Hz, 4H), 3.62 (t, ^{3}J = 5.3 Hz, 11H) [1H missing], 2.80 (t, ^{3}J = 5.8 Hz, 11H) [1H missing], 1.86 – 1.81 (m, 4H), 0.16 – 0.12 (dd, ^{3}J = 9.2, 6.8 Hz, 4H). ^{13}C NMR (101 MHz, $CDCl_3$) δ = 188.34, 163.30, 162.47, 145.23, 144.83, 137.12, 136.85, 134.68, 134.45, 129.17, 127.78, 126.52, 126.38, 119.09, 117.78, 67.63, 57.36, 56.51, 50.56, 29.19, 12.42.

1-(3-(-(1-(3-(silatranyl)propyl)-1H-1,2,3-triazol-4-yl)methoxy)phenyl)-3-(4-(-(1-(3-(silatranyl)propyl)-1H-1,2,3-triazol-4-yl)methoxy)phenyl)prop-2-en-1-one (CTSI 6): Yield: 81%; M. pt. < 220 ℃; Empirical formula: $C_{39}H_{52}N_8O_9Si_2$: Anal. Calcd: C, 56.2; H, 6.3; N, 13.5; Found: C, 56.3; H, 6.2; N, 13.5; IR (neat, cm^{-1}): 2933, 2872, 2807, 1655, 1596, 1508, 1480, 1438, 1381, 1350, 1303, 1244, 1172, 1122, 1096, 989, 938, 909, 831, 762, 680, 616, 583, 542. ^{1}H NMR (400 MHz, $CDCl_3$) δ = 7.69 – 7.61 (m, 2H), 7.61 – 7.56 (m, 2H), 7.55 – 7.52 (m, 1H), 7.52 – 7.43 (m, 2H), 7.26 (d, ^{1}J = 1.3 Hz, 2H), 7.22 (dd, ^{2}J = 5.0, 3.9 Hz, 1H), 7.14 (ddd, ^{3}J = 13.1, 10.6, 5.0 Hz, 2H), 5.16 (m, 3H) [1H missing], 4.70 (t, ^{3}J = 6.5 Hz, 1H), 4.24 (t, ^{3}J = 14.9 Hz, 4H), 3.65 (dd, ^{3}J = 12.1, 7.5 Hz, 11H) [1H missing], 2.75 – 2.68 (m, 12H), 1.92 – 1.86 (m, 4H), 0.31 – 0.28 (m, 4H). ^{13}C NMR (101 MHz, $CDCl_3$) δ = 186.13, 165.74, 162.49, 147.32, 140.50, 136.02, 133.56, 133.38, 134.65, 133.70, 132.30, 125.90, 120.60, 118.42, 117.86, 66.06, 57.31, 56.11, 51.11, 28.10, 11.33.

3-(2-(-(1-(3-(silatranyl)propyl)-1H-1,2,3-triazol-4-yl)methoxy)phenyl)-1-(4-(-(1-(3-(silatranyl)propyl)-1H-1,2,3-triazol-4-yl)methoxy)phenyl)prop-2-en-1-one (CTSI 7): Yield: 80%; M. pt. = 156 – 158 ℃; Empirical formula: $C_{39}H_{52}N_8O_9Si_2$: Anal. Calcd: C, 56.2;

H, 6.3; N, 13.5; Found: C, 56.1; H, 6.1; N, 13.6; IR (neat, cm^{-1}): 2946, 2873, 2807, 1656, 1597, 1507, 1454, 1338, 1303, 1275, 1245, 1213, 1168, 1122, 1095, 987, 938, 909, 933, 759, 678, 616,584, 572. ^{1}H NMR (400 MHz, DMSO) δ = 8.26 (s, 2H), 7.72 (s, 2H), 7.59 (dt, ^{3}J = 15.5, 7.1 Hz, 2H), 7.51 – 7.46 (m, 2H), 7.08 (d, ^{3}J = 8.9 Hz, 2H), 7.04 – 6.97 (m, 2H), 5.24 (s, 2H), 5.21 (s, 2H), 4.27 (dd, ^{3}J = 18.4, 7.2 Hz, 4H), 3.64 (dd, ^{3}J = 12.4, 6.0 Hz, 12H), 2.79 (dd, ^{3}J = 12.3, 6.0 Hz, 12H), 1.94 – 1.84 (m, 4H), 0.24 – 0.17 (m, 4H). ^{13}C NMR (101 MHz, $CDCl_3$) δ = 187.96, 165.23, 161.81, 148.00, 147.71, 143.81, 142.57, 136.12, 135.21, 135.02, 134.87, 133.70, 126.12, 124.63, 118.93, 117.83, 117.17, 116.12, 65.45, 57.50, 59.95, 51.55, 28.60, 11.84.

3-(3-(-(1-(3-(silatranyl)propyl)-1H-1,2,3-triazol-4-yl)methoxy)phenyl)-1-(4-(-(1-(3-(silatranyl)propyl)-1H-1,2,3-triazol-4-yl)methoxy)phenyl)prop-2-en-1-one (CTSI 8): Yield: 78%; M. pt. = 165 – 167 ℃; Empirical formula: $C_{39}H_{52}N_8O_9Si_2$: Anal. Calcd: C, 56.2; H, 6.3; N, 13.5; Found: C, 56.2; H, 6.3; N, 13.5; IR (neat, cm^{-1}): 2950, 2875, 2811, 1652, 1597, 1421, 1349, 1305, 1248, 1216, 1169, 1093, 1011, 910, 777, 721, 684, 541. ^{1}H NMR (400 MHz, $CDCl_3$) δ = 8.00 – 7.94 (m, 2H), 7.68 (d, ^{3}J = 15.6 Hz, 1H), 7.63 – 7.59 (m, 2H), 7.49 – 7.45 (m, 1H), 7.45 – 7.37 (m, 1H), 7.25 (d, ^{3}J = 8.0 Hz, 1H), 7.16 (d, ^{3}J = 7.6 Hz, 1H), 7.03 (s, 1H), 7.01 – 6.96 (m, 2H), 5.21 (s, 2H), 5.17 (s, 2H), 4.27 (t, ^{3}J = 7.5 Hz, 4H), 3.68 (t, ^{3}J = 5.8 Hz, 12H), 2.74 (t, ^{3}J = 5.8 Hz, 12H), 1.96 – 1.89 (m, 4H), 0.37 – 0.35 (m, 4H). ^{13}C NMR (101 MHz, $CDCl_3$) δ = 188.68, 162.23, 158.75, 143.74, 143.19, 142.72, 136.53, 132.10, 131.37, 130.86, 129.96, 128.51, 122.80, 122.28, 121.76, 114.72, 114.33, 62.32, 57.47, 53.48, 51.01, 26.34, 13.21.

1,3-bis(4-(-(1-(3-(silatranyl)propyl)-1H-1,2,3-triazol-4-yl)methoxy)phenyl)prop-2-en-1-one (CTSI 9): Yield: 83%; M. pt. = 173 – 175 ℃; Empirical formula: $C_{39}H_{52}N_8O_9Si_2$: Anal. Calcd: C, 56.2; H, 6.3; N, 13.5; Found: C, 56.3; H, 6.2; N, 13.3; IR (neat, cm^{-1}): 2949, 2876,

2811, 1655, 1597, 1508, 1438, 1350, 1305, 1248, 1215, 1168, 1096, 984, 909, 770, 721, 684, 645, 540. ^{1}H NMR (400 MHz, $CDCl_3$) δ = 7.65 (d, ^{3}J = 8.4 Hz, 1H) (1H missing), 7.55 (d, ^{3}J = 13.8 Hz, 2H), 7.46 (d, ^{3}J = 7.8 Hz, 2H), 7.31 (d, ^{3}J = 15.7 Hz, 2H), 6.92 (d, ^{3}J = 8.0 Hz, 2H), 6.47 (d, ^{3}J = 8.3 Hz, 1H), 6.41 (s, 1H), 5.16 (s, 2H), 4.07 (s, 2H), 3.65 (t, ^{3}J = 6.2 Hz, 12H), 2.75 (t, ^{3}J = 6.2 Hz, 12H), 1.77 – 1.73 (m, 4H), 0.34 – 0.30 (m, 4H). ^{13}C NMR (101 MHz, $CDCl_3$) δ = 195.53, 169.02, 165.28, 164.83, 148.54, 146.80, 137.73, 137.07, 134.97, 133.64, 130.28, 127.85, 127.38, 120.11, 110.16, 67.10, 60.74, 58.26, 57.52, 51.52, 29.19, 12.43.

Results and discussion

Synthesis of chalcone linked 1,2,3-triazole silatranes (CTSI 1–9)

The synthetic procedure followed for the generation of chemosensors **CTSI 1–9** has been summarized in Scheme 2. The final product generated in this four–step route, involves Claisen–Schmidt condensation followed by CuAAC reaction, as intermediary steps to generate organotriethoxysilanes (OTES). The final step proceeds by transetherification of OTES (1.0 equiv) with triethanolamine (1.0 equiv) using toluene as solvent and KOH as catalyst, resulting to caged silicon compounds **CTSI 1–9** that have been further explored for chemosensing studies. The resulting silatranes lock up silicon into a position difficult for water molecules[45] to disrupt silicon compounds and retain the structural properties of positional isomers.

Photophysical aspects

Procedure for UV–Vis/fluorescence study

UV–Vis spectroscopic data was collected using MeOH:H_2O (8:2) mixture as solvent system at 298 K within concentration range of 0.1 mM – 1 mM. Fluorescence properties were

explored for all **CTSI 1–9** under similar conditions, with 10 nm slit width and excitation wavelength of 307 and 311 nm, and at concentration of 10 μM. UV–Vis and fluorescence studies performed in methanolic–water solution of different isomers in quartz cell with path length of 1 cm. The quenching of different metal ions was explored stepwise using micro–syringe at different pH values and physiological temperature range.

Choice of solvent system

The chemosensing activity of an analyte in a particular solvent system is of primary importance as it determines its applicability in natural systems. The use of methanol as solvent was very effective for chemosensing activity but the aqueous environment was necessary to increase implementation to these ion detection studies. The choice of 'perfect solvent system' for chemosensing activity was explored using different permutations and combination of methanol and water (v/v) system in ratio 9:1, 8:2, 7:3, 6:4, 5:5 and 4:6. The different combinations were tested using fluorescence spectral response for CTSI 1 and are as shown in Figure 1. As water content in solvent system increases, the solubility of silatranes decreases, which precipitates out the analyte (silatrane) from the solution. This is evident from the change in coloration of analyte for different solvent systems as shown in Figure 1. The solution becomes progressively dilute for a given concentration, which is remarkably displayed by the decrease in emission intensity of fluorescence spectra for an analyte. After all these considerations, the best fit solvent system for effective chemosensing activity is 8:2 MeOH:H_2O combination.

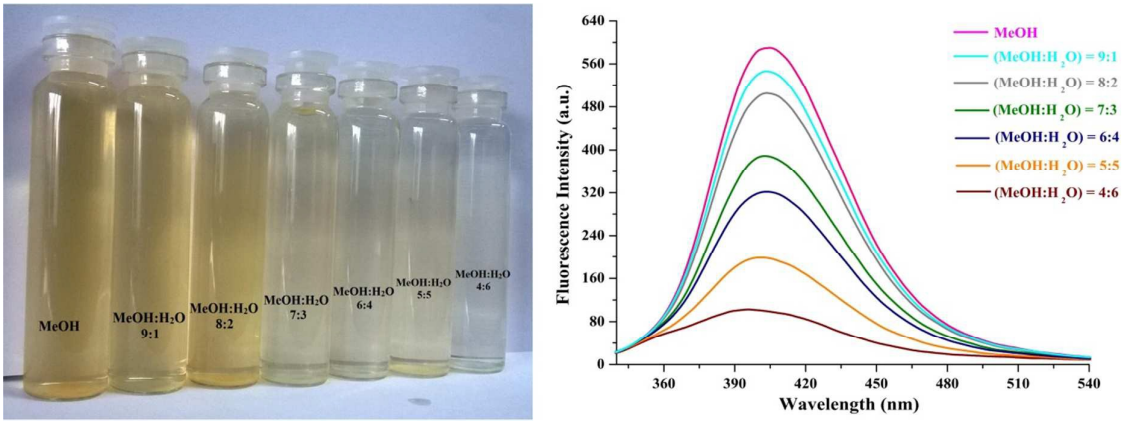

Figure 1: Sampling of **CTSI 1** in MeOH:H_2O (v/v) 10:0, 9:1, 8:2, 7:3, 6:4, 5:5 and 4:6 ration and; fluorescence spectral response using 20µM stock solution with λ_{ex} = 311 nm at 25 ℃

UV–Vis study

UV–Vis spectroscopic data recorded for 0.1 – 1.3 mM solution of **CTSI 1–9** is presented in Figure 2. UV–Vis spectra obtained after analysis displayed significant differences in absorption values for o-, m- and p-isomers. All CTS positional isomers exhibited major absorption band in the region 300 – 340 nm. The changes in $\boldsymbol{\lambda}_{max}$ value of UV–Vis spectra for different positional isomeric units impart uniqueness of each **CTS** isomer, as summarized in Table 1. It is noteworthy that with change in position of aldehyde substituent unit relevant to substituted acetophenones, a significant red shift was observed on moving from o→m→p position of isomers. The intensification in colour can be result of variation in position of auxochrome, which significantly affects spectra of chromophore. The change in polarity caused by –C=O auxochrome and decrease in steric hindrance resulted into red shift by 5 – 25 nm with shift in position from o→m→p position. Moreover, the conjugated electronic system absorbs at maximum intensity when in planar configuration and tends to have higher values of $\boldsymbol{\lambda}_{max}$ and molar absorptivity co-efficient $\boldsymbol{\varepsilon}_{max}$.

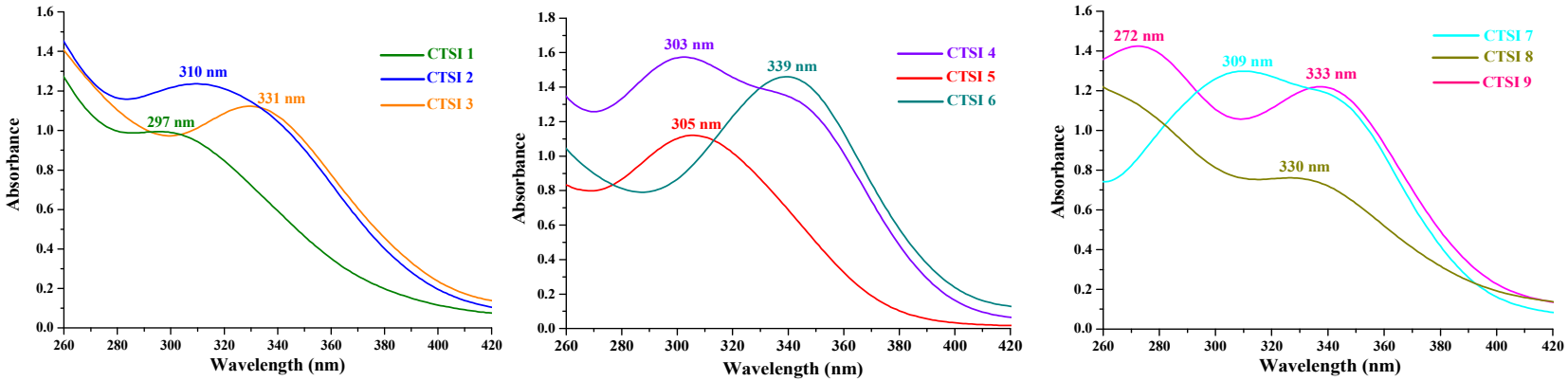

Figure 2: UV–Vis spectra of **chalcomers 1–9** (0.5 – 0.6 mM for CTSI **1–3**; 1.2 – 1.3 mM for CTSI **4–6** and 1.0 – 1.2 mM for CTSI **7–9**) in MeOH:H_2O (8:2) (v/v) solvent system at 25 ℃

CTS isomer	1	2	3	4	5	6	7	8	9
λ_{max} (nm)	297	310	331	303	305	339	309	330	333
ε_{max} (x 10^4)	5.94	5.17	6.02	2.53	2.34	2.61	2.81	2.75	2.78

Table 1: Molar absorptivity co-efficient (ε_{max}) ($moldm^{-3}$) of chalcomers **1–9** calculated using path length of 1 cm and solution concentration in the range 0.1 – 1.3 mM in MeOH:H_2O (8:2) (v/v) solvent system at 25 ℃

Molar absorptivity

UV–Vis spectra recorded in 8:2 (v/v) methanol–water solution at the concentration of 5–6 x 10^{-4} M for **CTSI 1–3**, 12–13 x 10^{-4} M for **CTSI 4–6** and 10–12 x 10^{-4} M for **CTSI 7–9** show large variations in molar absorptivity coefficient (ε_{max}). The calculations show the difference in activity of each chalcone linked 1,2,3-triazolyl positional isomer. The o-isomer of aldehyde show large value of molar extinction coefficient as compared to their m- and p-positional isomers (Table 1). This phenomenon is observed due to the localized elongation in π–electronic conjugate system.

Concentration variation in UV–Vis spectra

The influence of concentration change on λ_{max} value of absorption spectra for **CTSI 9** and is represented in Figure 3. The spectra revealed a strong change in absorption intensity arising at 269 nm with a moderate change in intensity for peak at 333 nm. The increase in **CTSI 9** concentration is associated with hypsochromic shift of 7 nm, from 340 to 333 nm while no shift for peak at 269 nm was observed. This absorption maxima resulted from increased conjugation causes blue shift in absorption maxima which is due of lowering of energy levels for both excited and ground states. There was minimal change in absorption spectra with variation in concentration for other chalcomers.

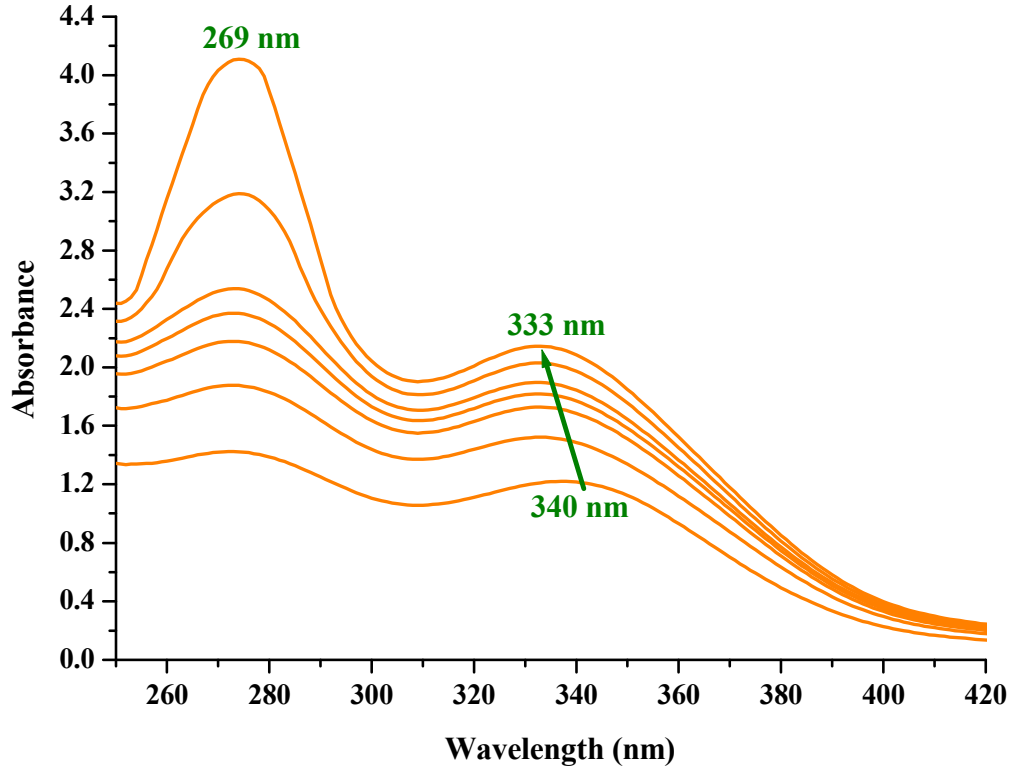

Figure 3: Effect of concentration variation on **CTSI 9** (1 – 10 equiv) in MeOH:H_2O (8:2) (v/v) system at 25 ℃

Florescence spectral study

Fluorescence spectral measurements

In this report, we describe the synthesis and applicability of new type of fluorescent isomeric chemosensors that provide selectivity in fluorescence quenching. Among the nine chalcone isomers used in study, only three o-positional isomers were found to be active in fluorescence quenching studies. **CTSI 1–3** exhibited excellent fluorescence maxima at concentration of 10 μM and show considerable activity till threshold concentration level of 50 nM. The remaining **CTSI 4–9** were inactive to fluorescence spectral studies (Figure 4). In previous reports,

regarding the sensing of Cu^{2+} and Ni^{2+} independently, the minimum analyte concentration required for the efficient sensing lie between 20 – 50 µM.[19–24] This positional isomeric effect on emission spectra is consequence of ***O,O,N*** and ***N,O, –C=C–*** coordinating sphere that can effectively bind Cu^{2+} and Ni^{2+} ions in o-isomers (**CTSI 1–3**) (Scheme 3). This spatial environment of rigid donor atom is lacking in the case of m- and p- isomers (**CTSI 4–9**).

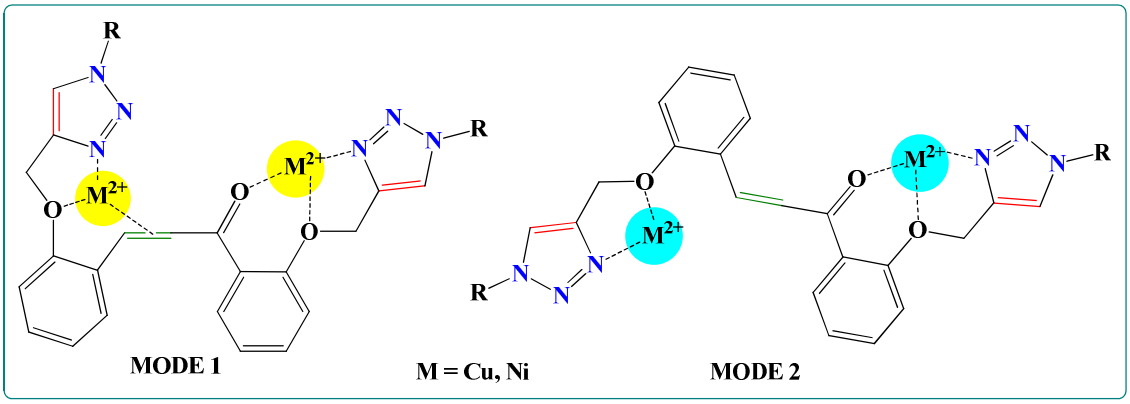

Scheme 3: Proposed binding modes for **CTSI 1–3** for interactions with Cu^{2+} and Ni^{2+} ions

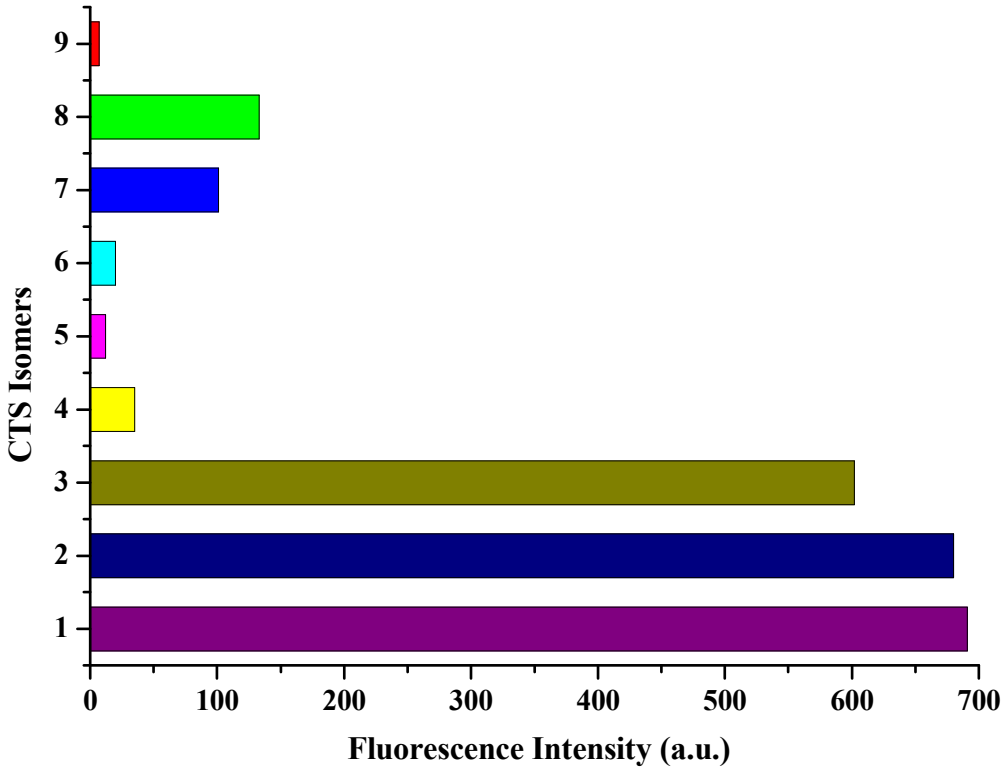

Figure 4: Fluorescence emission spectra of CTSI **1–9** in MeOH:H_2O (8:2) (v/v) system at concentration of 10 μM and λ_{ex} = 311 nm at 25 ℃

Selectivity over various cations

The ability of conjugated system to complex with transition elements has provided the basis for spectro-chemical analysis using fluorescence technique. The stock solutions were prepared by dissolving **CTSI 1–3** in (8:2) methanolic–water solution at the concentration level of 20 μM. The cationic stocks too were prepared in MeOH:H_2O (8:2) concentration level of 10 μM. The fluorescence quenching was studying using chloride ion salts of Hg^{2+}, Cd^{2+}, Cr^{2+}, Cu^{2+}, Ca^{2+}, Na^{+}, Mg^{2+}, Zn^{2+}, Ni^{2+}, Rb^{+}, Ba^{2+}, Ag^{+}, Fe^{2+} and Fe^{3+} ions (Figure 5). The binding affinities towards these cations show unrecognizable changes in spectral

intensity, with exception of Cu^{2+} and Ni^{2+} that show significant quenching in fluorescence emission spectral intensity.

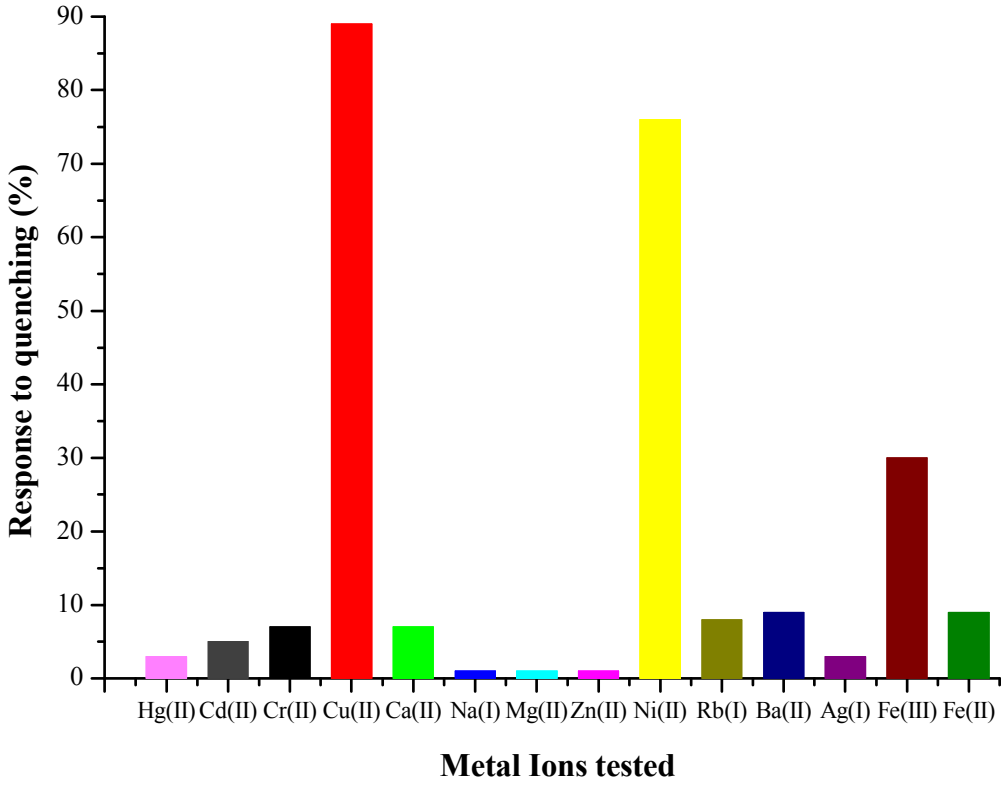

Figure 5: Chemosensing activity of probe **CTSI 1** towards different cationic species in MeOH:H_2O (8:2) (v/v) solution after the addition of 5.0 equiv of Hg^{2+}, Cd^{2+}, Cr^{2+}, Cu^{2+}, Ca^{2+}, Na^{+}, Mg^{2+}, Zn^{2+}, Ni^{2+}, Rb^{+}, Ba^{2+}, Ag^{+}, Fe^{2+} and Fe^{3+}, respectively with λ_{ex} = 311 nm at 25 ℃

Detection limits

Fluorescence spectroscopic measurements were recorded in the range 390 – 420 nm, with excitation wavelength for absorption maxima lying in the region of 307 – 311 nm. The emission value in this region is popularly referred to as Soret band. The titration studies were

performed for **CTSI 1–3** with Cu^{2+} and Ni^{2+} ions at concentration level of 15 μmol/L and 20 μmol/L, respectively. The recognition studies were performed to evaluate threshold concentration values for chemosensor and the minimum detection limits for these cationic quenchers.

Quenching study

The detection of metal ions by a fluorescent chemosensor is based upon two techniques that involve either quenching in emission maxima or enhancement of fluorescence intensity. The decrease in intensity on complexation with metal ions is due to the decrease in rigidity of conjugated π electrons and the sharing of electron cloud with metal ions. While the increase in intensity of fluorescence maxima is due to more stable and rigid system that results into increased quantum yield of a system. The development of spectrometric studies is due to the movement of electrons between different energy levels of organometallic complexes by the energy provided by UV or visible light.[7]

Cu^{2+} and Ni^{2+} ions show significant quenching in fluorescence spectra of **CTSI 1–3** while other metal ions show negligible changes. The emission intensity decreased rapidly with addition of 10 – 25 equiv of both Cu^{2+} (Figure 6–8) and Ni^{2+} (Figure 9–11) cationic binders. Thereafter, no decrease in emission was evident, which indicated the saturation of active fluorophore sites by quencher cationic species. Thus, ratiometric sensing of Cu^{2+} and Ni^{2+} ions fall within the physiologically relevant concentration range.

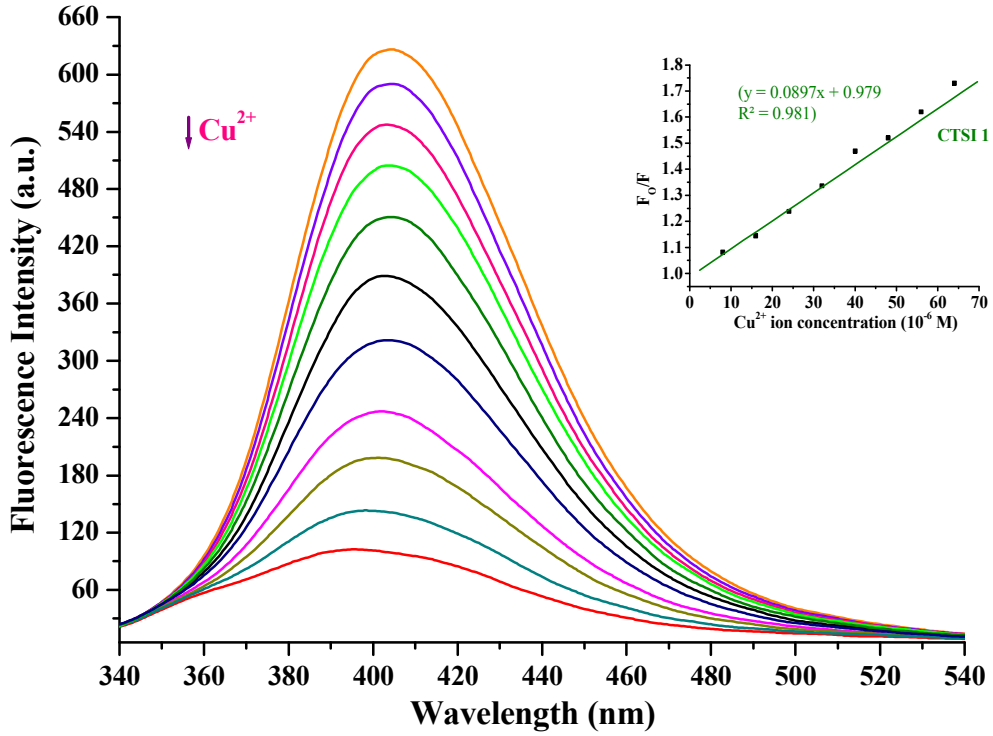

Figure 6: Fluorescence emission spectra and variation of fluorescence quenching (inset) recorded using Stern–Volmer plot for **CTSI 1** (10 μM) upon gradual addition of Cu^{2+} (0 – 20 equiv) in MeOH:H_2O (v/v) (8:2) with λ_{ex} = 311 nm

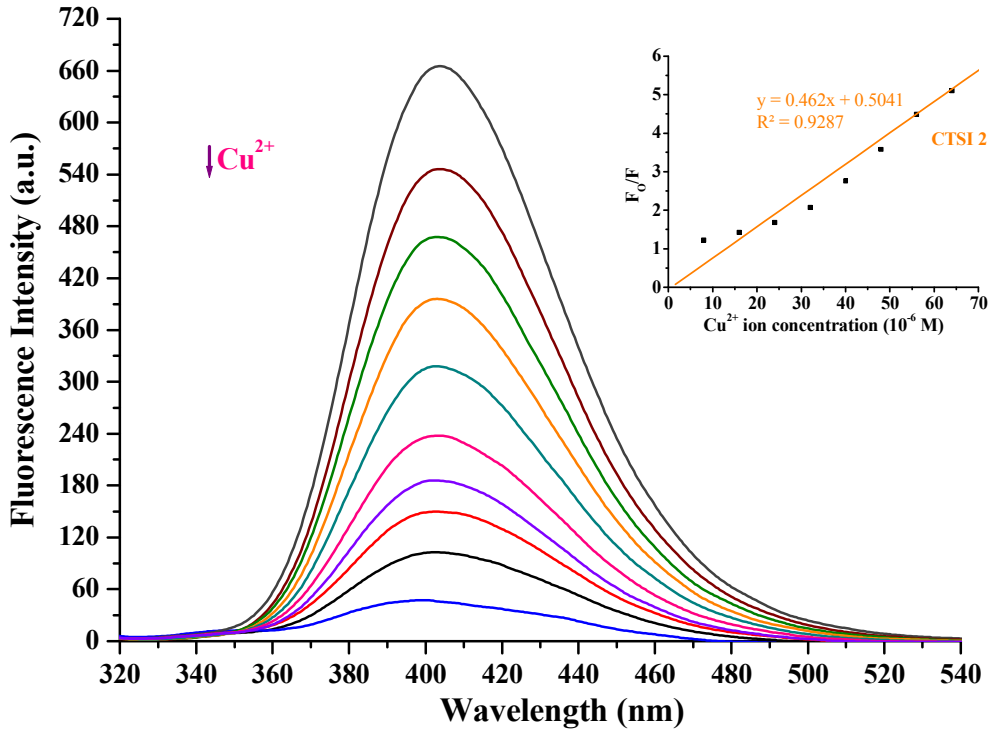

Figure 7: Fluorescence emission spectra and variation of fluorescence quenching (inset) recorded using Stern–Volmer plot for **CTSI 2** (10 μM) upon gradual addition of Cu^{2+} (0 – 20 equiv) in MeOH:H_2O (v/v) (8:2) with λ_{ex} = 311 nm

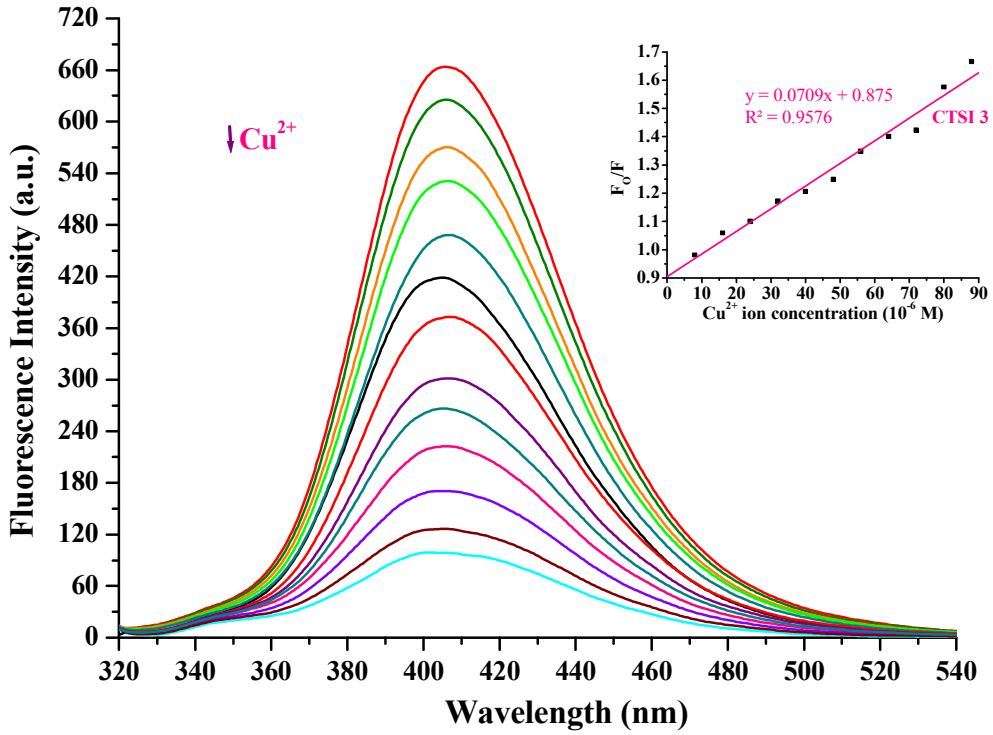

Figure 8: Fluorescence emission spectra and variation of fluorescence quenching (inset) recorded using Stern–Volmer plot for **CTSI 3** (10 μM) upon gradual addition of Cu^{2+} (0 – 20 equiv) in MeOH:H_2O (v/v) (8:2) with λ_{ex} = 311 nm

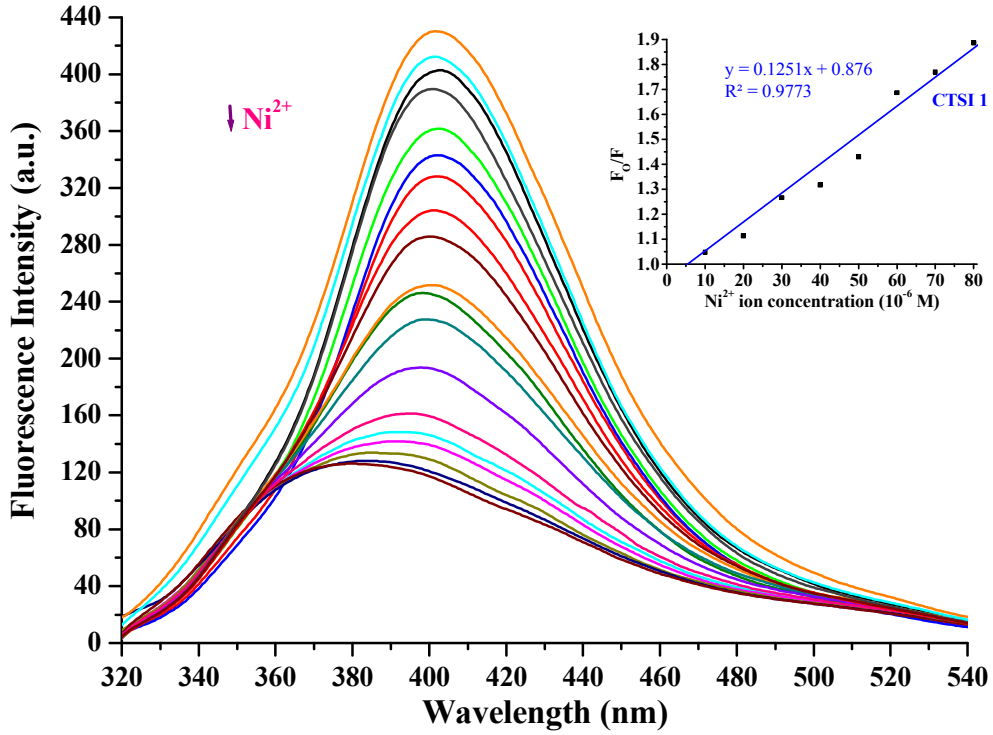

Figure 9: Fluorescence emission spectra and variation of fluorescence quenching (inset) recorded using Stern–Volmer plot for **CTSI 1** (10 μM) upon gradual addition of Ni^{2+} (0 – 30 equiv) in MeOH:H_2O (v/v) (8:2) with λ_{ex} = 307 nm

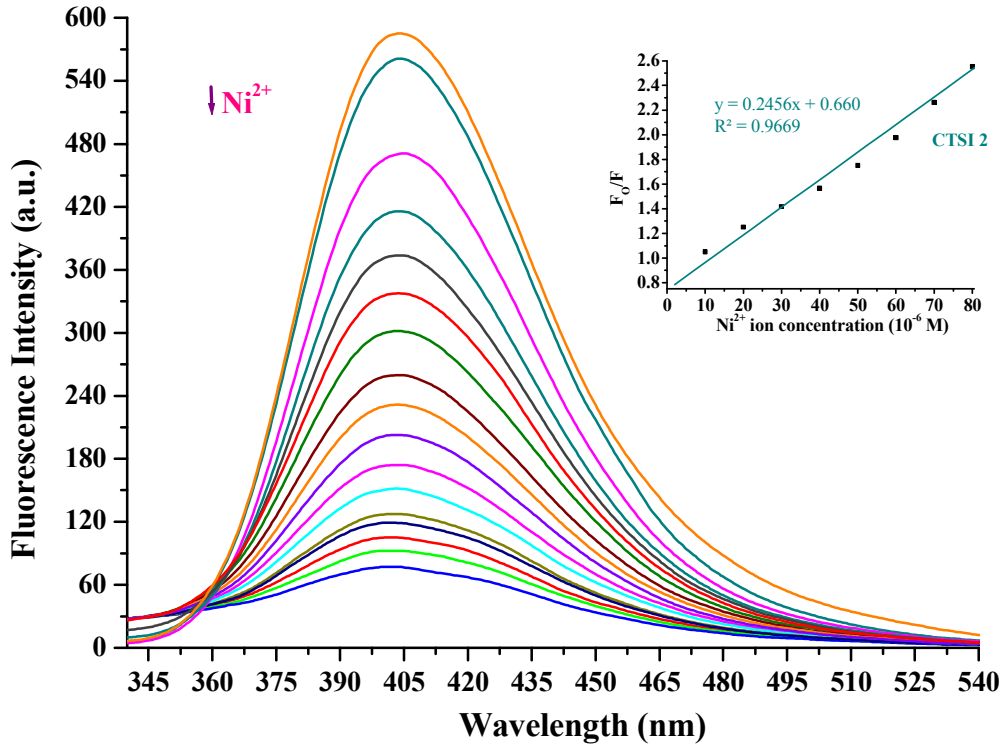

Figure 10: Fluorescence emission spectra and variation of fluorescence quenching (inset) recorded using Stern–Volmer plot for **CTSI 2** (10 μM) upon gradual addition of Ni^{2+} (0 – 30 equiv) in MeOH:H_2O (v/v) (8:2) with λ_{ex} = 307 nm

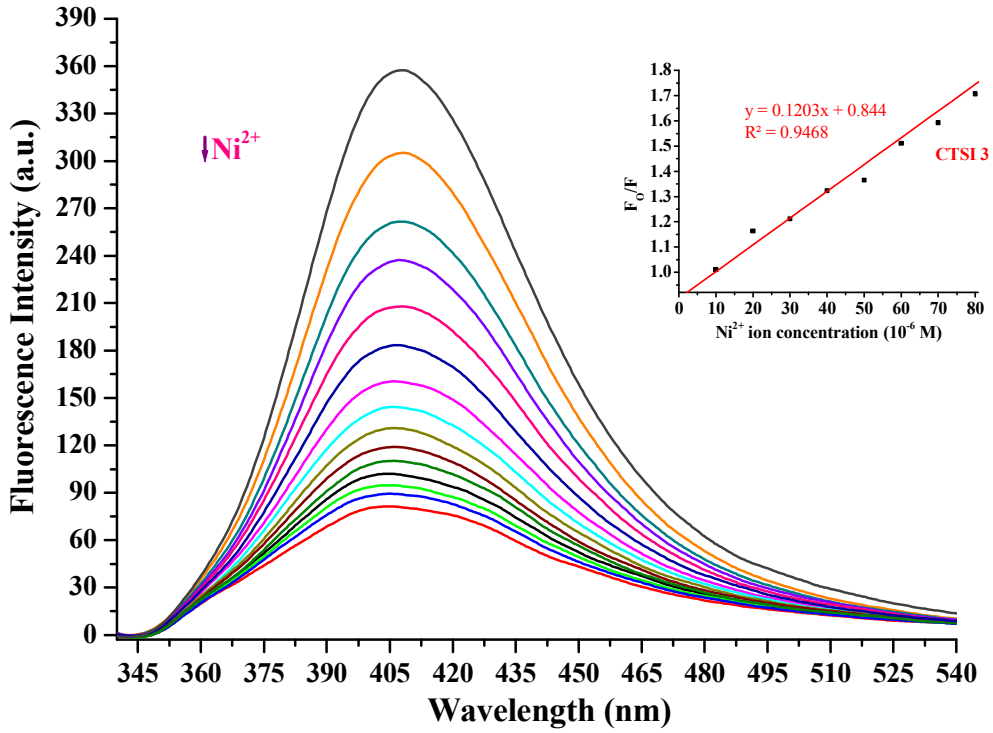

Figure 11: Fluorescence emission spectra and variation of fluorescence quenching (inset) recorded using Stern–Volmer plot for **CTSI 3** (10 μM) upon gradual addition of Ni^{2+} (0 – 30 equiv) in MeOH:H_2O (v/v) (8:2) with λ_{ex} = 307 nm

However, a straight turn-on fluorescent sensor is much harder to obtain than a turn-off sensor. Interestingly, **CTSI 8** shows exceptional property to acts as 'turn on' fluorescent sensor for Ni^{2+} ions irrelevant to presence of other cationic species. There was increase in fluorescence intensity upon addition of 15 μM methanolic solution of Ni^{2+} ions. This prototype for 'turn-on' fluorescence probe with Ni^{2+} ions was distinctive from other chalcomers studied (**CTSI 1–3**) (Figure 12).

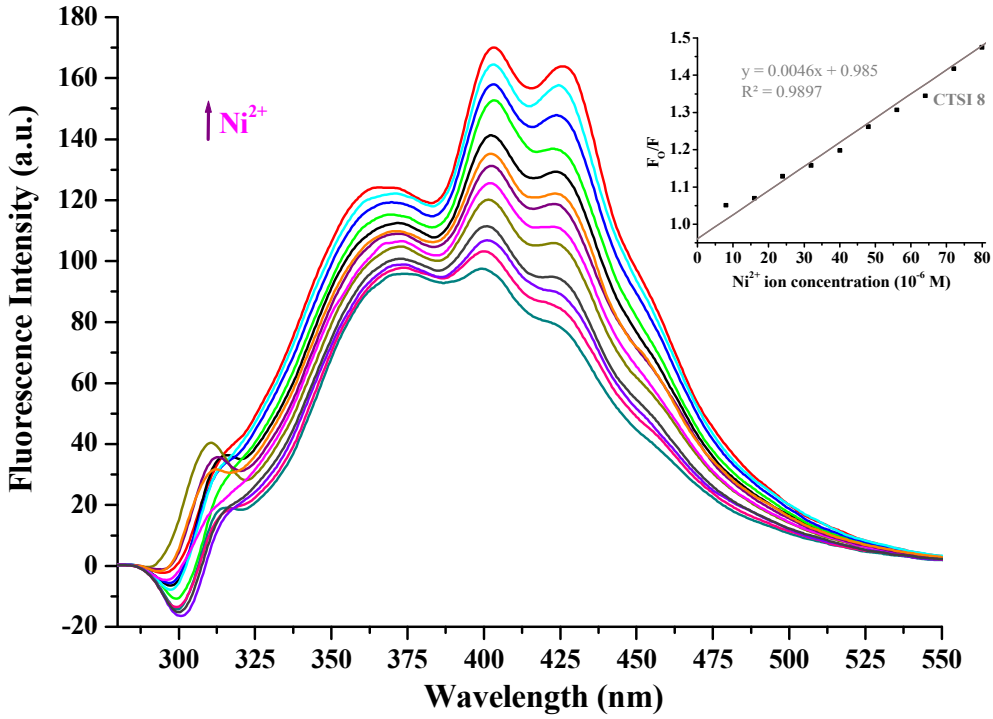

Figure 12: Fluorescence emission spectra and variation of fluorescence quenching (inset) recorded using Stern–Volmer plot for **CTSI 8** (30 μM) upon gradual addition of Ni^{2+} (0 – 50 equiv) in MeOH:H_2O (v/v) (8:2) with λ_{ex} = 311 nm

It is worth noting that the behavior observed for Cu^{2+} and Ni^{2+} ion sensing is similar to that reported in previous studies.[20,46] However, in contrast with known literature, chalcone based sensor system is more efficient in fluorescent detection of Cu^{2+} and Ni^{2+} ions with threshold sensing concentration of as low as 10 μM. Moreover, there is no single system, to the best of knowledge, that can competently sense both Cu^{2+} and Ni^{2+} ions in 20% aqueous media (8:2, MeOH:H_2O). Further, with the evidence of considerable quenching observed for **CTSI 1–3** in the case of Cu^{2+} and Ni^{2+} ions, **CTSI 8** resulted into the enhancement of fluorescence maxima with addition of Ni^{2+} ion solution showing no effect with Cu^{2+} ions, which is unique for mono analyte sensor system.

Stern–Volmer constant

The Stern–Volmer plot for quencher concentration for all fluorescence active chalcomers as shown in Figure 13. The non–linearity in plots shows that the quenching is due to heterogeneous dispersion of chromophore in the solution matrix. Moreover, the binding of transition metal ions occur in ground state by the process called static quenching. The graph shows higher Stern–Volmer constant (K_{SV}) for o-isomer in comparison to other isomers which demonstrates higher quenching ability of o-isomer as compared to their m- and p-substituted isomers in case of both Ni^{2+} and Cu^{2+} ions.

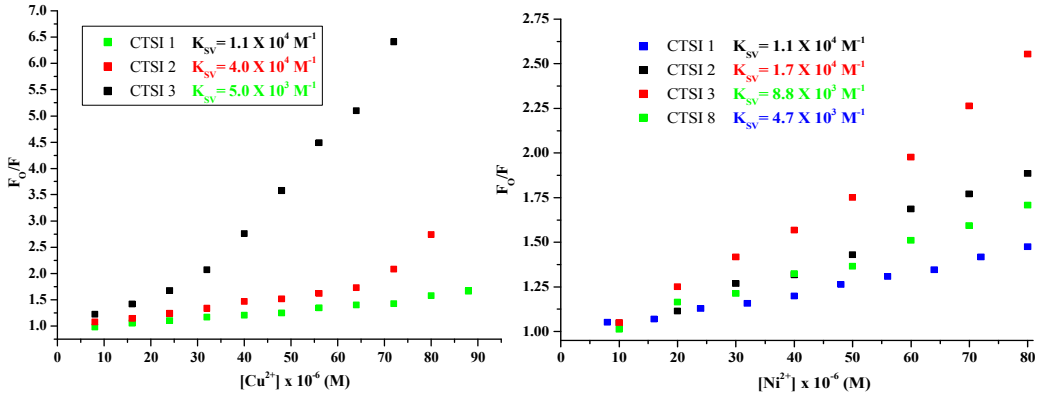

Figure 13: Stern–Volmer plots for different Chalcomers in response to Ni^{2+} and Cu^{2+} ions in concentration range of 10 – 50 µM at 25 ℃

pH effect

The effect of pH change on emission maxima illustrated the variation in fluorescence intensity recorded in the range of 5 – 13 (Figure S1). So far no literature has been reported citing the effect of pH on sensing of Cu^{2+} and Ni^{2+} ions, as the studies were performed using buffer solutions. The gradual change in pH from acidic to basic (5 – 13) resulted into steady

increase in emission maxima. The spectral maxima become constant after pH of 11 and any further increase in pH results into decrease in emission wavelength (λ_{ems}) value. Therefore, the pH range for fluorescence study lies in the range 5 – 9.

A series of fluorescence titrations were performed on **CTSI 1** to study the effect of pH on quenching activity of probe towards Cu^{2+} and Ni^{2+} ions. This is illustrated by the increase in fluorescence emission maxima that arises due to increase in hydration shells of Cu^{2+} and Ni^{2+} ions (Figure S2). Initializing, our study from pH of 5, emission intensity was obtained at 430 nm with λ_{ext} at 311 nm. With the rise in pH to 7, a slight increase in fluorescence intensity pointed towards the decrease in sensing of quencher cations by the probe. On raising solution pH to 11, there was decrease in emission intensity that point out to the alteration in probe–sensor activity of binding module.

Temperature effect

The ion recognition studies for **CTSI 1** show significant effect of temperature change on quenching phenomenon. The chemosensing activity of fluorophore was explored within the temperature range of 298 K to 328 K (Figure S3) which falls within physiological temperature range. On raising the temperature of solution from 298 K to 308 K, there is noticeable increase in quenching of emission maxima. With further 10º rise in temperature, there was still increase in quenching for both cationic species. Further raising temperature by 10º, considerable change in quenching was evident. Lowering thermal activity with decrease in solution temperature from 298K to 288K, a marginal dip in quenched maxima was observed. Thus, the optimal thermal condition for fluorescence titration studies that lie within the physiological temperature of range 298 K to 318 K.

Conclusion

The efficient synthesis of chalcomers linked to capped silicon via 1,2,3-triazolyl propyl chain is being reported for first time. Higher values of molar extinction coefficient in case of all chalcone isomeric units show the high absorption in UV–Vis spectra. The exceptional sensing ability of o-isomer of CTS over their m- and p-isomeric analogues towards Cu^{2+} and Ni^{2+} ions show key difference in photophysical properties arising due to positional isomerism. This dual sensing behaviour resulted in the quenching of emission spectral maxima due to Cu^{2+} and Ni^{2+} ions. In contrast, **CTSI 8** has a remarkable property to sense of Ni^{2+} ions as 'turn on' fluorescent sensor. The optimal conditions for fluorescent chemosensing lie within physiologically relevant conditions with pH range of 5 – 9 and temperature variation of 288 – 318 K. Moreover, the assembled chalcomer silatranes can extend their scope to medicine with further advancement as Cu^{2+} and Ni^{2+} cationic sensors.

Acknowledgments

We thank Mr. Avtar Singh and Mr. Manish Kumar for the NMR studies (SAIF, Panjab University, Chandigarh). One of the authors, Jandeep Singh thanks Council of Scientific and Industrial Research (CSIR), India for providing financial support in the form of CSIR–SRF (NET) fellowship.

Notes

The authors declare no competing financial interest.

References

1 T. Daniel Thangadurai, G. Chung, O. Kwon, D. Jin, and Y. I. Lee, *Tetrahedron Lett.*, 2011, **52**, 6465–6469.

2 S. Kubow, *J. Nutr. Biochem.*, 1996, **7**, 530–541.

3 E. Schmitt, I. C. Tanrikulu, T. H. Yoo, M. Panvert, D. A Tirrell, and Y. Mechulam, *J. Mol. Biol.*, 2009, **394**, 843–851.

4 K. P. Carter, A. M. Young, and A. E. Palmer, *Chem. Rev.*, 2014, **114**, 4564–4601.

5 T. Slezak, Z. M. Smith, J. L. Adcock, C. M. Hindson, N. W. Barnett, P. N. Nesterenko, and P. S. Francis, *Anal. Chim. Acta*., 2011, **707**, 121–127.

6 M. Li, H. Gou, I. Al-ogaidi, and N. Wu, 2013, *ACS Sustainable Chem Eng.*, 2013, **1**, 713–723.

7 M. Dutta and D. Das, *TrAC Trends in Anal. Chem.*, 2012, **32**, 113–132.

8 M. Y. Berezin and S. Achilefu, *Chem. Rev.*, 2010, **110**, 2641–2684.

9 M. A Saeed, H. T. M. Le, and O. Š. Miljanić, *Acc. Chem. Res*., 2014, **47**, 2074–2083.

10 H. Kim and H. Choi, *Talanta*, 2001, **55**, 163–169.

11 H. N. Kim, Z. Guo, W. Zhu, J. Yoon, and H. Tian, *Chem. Soc. Rev.,* 2011, **40**, 79–93.

12 Z. Liu, W. He, and Z. Guo, *Chem. Soc. Rev., 2*013, **42**, 1568–1600.

13 M. Swierczewska, S. Lee, and X. Chen, *Phys. Chem. Chem. Phys.*, 2011, **13**, 9929–9941.

14 N. Boens, V. Leen, and W. Dehaen, *Chem. Soc. Rev.,* 2012, **41**, 1130–1172.

15 E. Denkhaus and K. Salnikow, *Crit. Rev. in onco./hemato.*, 2002, **42**, 35–56.

16 D. E. Kang, C. S. Lim, J. Y. Kim, E. S. Kim, H. J. Chun, and B. R. Cho, *Anal. Chem.*, 2014, **86**, 5353–5359.

17 Y. Rahimi, A. Goulding, S. Shrestha, S. Mirpuri, and S. K. Deo, *Biochem. Biophys. Res. Commun.*, 2008, **370**, 57–61.

18 J. Ding, L. Yuan, L. Gao, and J. Chen, *J. Lumin.*, 2012, **132**, 1987–1993.

19 S. Ramakrishnan, E. Suresh, A. Riyasdeen, M. A. Akbarsha, and M. Palaniandavar, *Dalton Trans.*, 2011, **40**, 3245–56.

20 P. Krishnamoorthy, P. Sathyadevi, R. R. Butorac, A. H. Cowley, N. S. P. Bhuvanesh, and N. Dharmaraj, *Dalton Trans.*, 2012, **41**, 4423–4436.

21 J. Tan, L. Zhu, and B. Wang, *Dalton Trans.*, 2009, **2**, 4722–4728.

22 H. Wang, D. Wang, Q. Wang, X. Li, and C. A Schalley, *Org. Biomol. Chem.*, 2010, **8**, 1017–26.

23 G. Singh, J. Singh, S. S. Mangat, and A. Arora, *Tetrahedron Lett.*, 2014, **55**, 2551–2558.

24 J. Tatsuzaki, K. F. Bastow, K. Nakagawa-Goto, S. Nakamura, H. Itokawa, and K.-H. Lee, *J. Nat. Prod.*, 2006, **69**, 1445–1449.

25 F. Chimenti, R. Fioravanti, A. Bolasco, P. Chimenti, D. Secci, F. Rossi, M. Yáñez, F. Orallo, F. Ortuso, and S. Alcaro, *J. Med. Chem.*, 2009, **52**, 2818–2824.

26 M. N. Clifford, and F. A. Toma, *J. Sci. Food Agric.*, 2000, **1080**, 1073–1080.

27 A. Sharma, B. Chakravarti, M. P. Gupt, J. a Siddiqui, R. Konwar, and R. P. Tripathi, *Bioorg. Med. Chem.*, 2010, **18**, 4711–4720.

28 H. Sharma, S. Patil, T. W. Sanchez, N. Neamati, R. F. Schinazi, and J. K. Buolamwini, *Bioorg. Med. Chem.*, 2011, **19**, 2030–2045.

29 Z. Nowakowska, *Eur. J. Med. Chem.*, 2007, **42**, 125–137.

30 H. Jin, X. Li, T. Tan, S. Wang, Y. Xiao, and J. Tian, *Dyes Pigm.*, 2014, **106**, 154–160.

31 K. Namba, A. Osawa, S. Ishizaka, N. Kitamura, and K. Tanino, *J. Am. Chem. Soc.*, 2011, **133**, 11466–11469.

32 Q. Shen, L. Zhou, Y. Yuan, Y. Huang, B. Xiang, C. Chen, Z. Nie, and S. Yao, *Biosens. Bioelectron.*, 2014, **55**, 187–194.

33 M. Meldal and C. W. Tornøe, *Chem. Rev.*, 2008, **108**, 2952–3015.

34 N. Boechat, V. F. Ferreira, S. B. Ferreira, M. de Lourdes G Ferreira, F. de C da Silva, M. M. Bastos, M. Dos S Costa, M. C. S. Lourenço, A. C. Pinto, A. U. Krettli, A. C. Aguiar, B. M. Teixeira, N. V da Silva, P. R. C. Martins, F. A. F. M. Bezerra, A. L. S. Camilo, G. P. da Silva, and C. C. P. Costa, *J. Med. Chem.*, 2011, **54**, 5988–99.

35 G. Acquaah-harrison, S. Zhou, J. V Hines, and S. C. Bergmeier, *J. Comb. Chem.*, 2010, 491–496.

36 S. B. Ferreira, A. C. R. Sodero, M. F. C. Cardoso, E. S. Lima, C. R. Kaiser, F. P. Silva, and V. F. Ferreira, *J. Med. Chem.*, 2010, **53**, 2364–2375.

37 G. Singh, S. S. Mangat, H. Sharma, J. Singh, A. Arora, A. P. Singh Pannu, and N. Singh, *RSC Adv.*, 2014, **4**, 36834– 36844.

38 G. Singh, S. S. Mangat, J. Singh, A. Arora, and R. K. Sharma, *Tetrahedron Letters*, 2014, **55**, 903–909.

39 G. Singh, S. S. Mangat, J. Singh, A. Arora, and M. Garg, *J. Organomet.Chem.*, 2014, **769**, 124–129.

40 G. Singh, A. Arora, S. S. Mangat, J. Singh, S. Chaudhary, N. Kaur, and D. Choquesillo-Lazarte, *J. Molec.r Stuct.*, 2015, **1079**, 173–181.

41 G. Singh, J. Singh, S. S. Mangat, A. Arora, *RSC Adv.*, 2014, DOI: 10.1039/C4RA08724K.

42 A. T. Dickschat, F. Behrends, M. Bühner, J. Ren, M. Weiss, and H. Eckert, A. Studer, *Chem. Eur. J.*, 2012, **18**, 16689–16697.

43 K. W. Huang, C. W. Hsieh, H. C. Kan, M. L. Hsieh, S. Hsieh, L. K. Chau, T. E. Cheng, and W. T. Li,. *Sens Actuators, B*, 2012, **163**, 207–215.

44 A. Bianco, M. Maggini, M. Nogarole, and G. Scorrano, *Eur. J. Org. Chem.*, 2006, 2934–2941.

45 a) H. F. Sore, W. R. J. D. Galloway, and D. R. Spring, *Chem. Soc. Rev.*, 2012, **41**, 1845–66. b) L. Huerta, J. El Haskouri, D. Vie, M. Comes, J. Latorre, C. Guillem, M. D. Marcos, D. Beltra, and P. Amoro, *Chem. Mater.*, 2007, **19**, 1082–1088. c) K. Ladomenou, T. N. Kitsopoulos, G. D. Sharma, and a. G. Coutsolelos, *RSC Adv.*, 2014, **4**, 21379.

46 T. Mukherjee, J. C. Pessoa, A. Kumar and A. R. Sarkar, *Dalton Trans.*, 2013, **42**, 2594–2607.